frontiers | Frontiers in Ecology and Evolution

ORIGINAL RESEARCH
published: 14 April 2022
doi: 10.3389/fevo.2022.721244

Physiological Responses of Typical Wetland Plants Following Flooding Process—From an Eco-Hydrological Model Perspective

Chengliang Liu[1], Yijian Zeng[1], Zhongbo Su[1] and Demin Zhou[2,3]**

[1] Department of Water Resources, Faculty of Geo-Information Science and Earth Observation, University of Twente, Enschede, Netherlands, [2] College of Resource Environment and Tourism, Capital Normal University, Beijing, China, [3] Key Laboratory of 3D Information Acquisition and Application of Ministry, Capital Normal University, Beijing, China

OPEN ACCESS

Edited by:
Carlos Freitas, Federal University of Amazonas, Brazil

Reviewed by:
Yu An, Northeast Institute of Geography and Agroecology (CAS), China
Ji-Zhong Wan, Qinghai University, China

***Correspondence:**
Zhongbo Su
z.su@utwente.nl
Demin Zhou
zhoudemin@cnu.edu.cn

Specialty section:
This article was submitted to Conservation and Restoration Ecology, a section of the journal Frontiers in Ecology and Evolution

Received: *06 June 2021*
Accepted: *07 March 2022*
Published: *14 April 2022*

Citation:
Liu C, Zeng Y, Su Z and Zhou D (2022) Physiological Responses of Typical Wetland Plants Following Flooding Process—From an Eco-Hydrological Model Perspective. Front. Ecol. Evol. 10:721244. doi: 10.3389/fevo.2022.721244

Anaerobics increase resistance to gas transport and microbial activity in flooded soils. This may result in the presence of aerenchyma in the roots of some wetland plants. Increased aerenchyma airspaces enable oxygen to be transported from the above-ground plant parts to the submerged roots and rhizosphere. Nevertheless, there is still a lack of studies linking field experiments and eco-hydrological modeling to the parameterization of the physiological responses of typical wetland plant species to natural flooding events. Furthermore, from the modeling perspective, the contribution of aerenchyma was not sufficiently considered. The goal of this study was to develop and apply an eco-hydrological model capable of simulating various patterns of plant physiological responses to natural flooding events based on key processes of root oxygen diffusion and aerenchyma functioning in a variably-saturated wetland soil environment. Eco-hydrological experiments were conducted accordingly, with surface water level, root-zone soil water content, soil temperature, leaf net photosynthesis rate and root morphology monitored simultaneously *in situ* at a site dominated by meadow species *Deyeuxia angustifolia* (Kom.) Y. L. Chang and invaded shrub species *Salix rosmarinifolia* Linn. var. *brachypoda* (Trautv.et Mey.) Y.L. Chou in a typical natural floodplain wetland. The results are as follows: (1) Root oxygen respiration rates are strongly correlated with leaf net photosynthesis rates of the two plant types, particularly under flooding conditions during the growing season; (2) Meadow species with a preference for wet microhabitats has a competitive advantage over first-year invading shrub species during flooding events; and (3) an aerenchyma sub-model could improve the eco-hydrological model's accuracy in capturing plant physiological responses. These findings have the potential to contribute to the management of wetland and its restorations.

Keywords: soil water dynamics, riparian habitat, inland wetlands, flooding, photosynthesis, root oxygen respiration

INTRODUCTION

Along flooding gradients, plant zonation is widely observed and extensively described (Ewing, 1996; Zhou et al., 2009, 2013; Kirwan and Guntenspergen, 2015; Pedersen et al., 2017; Haak et al., 2017; Wright et al., 2017). Typically, plant zonation is attributed to differences in flood tolerance, more specifically, the ability of plants to tolerate hypoxic rooting conditions (Armstrong et al., 1994; Reddy and DeLaune, 2008). The hydrological regime, particularly the dynamics of the water table due to seasonal flooding, has an effect on soil features by regulating the area and duration of saturation (Rubol et al., 2012), which indicates the occurrence and intensity of anaerobic soil conditions. The primary constraint imposed by flooding on wetland plants is the exchange of gas. In flooded soils, anaerobics improve resistance to gas transportation and microbial activities. This could occur in a matter of hours in freshly flooded soils. The impact could also be accelerated at high temperatures (Armstrong et al., 2000).

Seasonal flooding tolerance is characterized by distinct physiological features include, among others, leaf net photosynthesis rate (LNPR) (Pezeshki, 2001; Dalmagro et al., 2016), aerenchyma abundance (Laan et al., 1989; Wright et al., 2017), and root oxygen respiration (Armstrong et al., 2019). The amount of internal oxygen in plants depends both on the root respiration rate and the soil microbe respiration (Kumari and Gupta, 2017). Root oxygen respiration is crucial for maintaining vital physiological and metabolic pathways (Glenz et al., 2006), particularly in wetland plants. Leaf photosynthesis is a critical physiological activity because it directly reflects the ability of growth and nutrient absorption (Lai et al., 2012; Pezeshki et al., 2018). It was found that a significant portion of the oxygen diffusing to the roots during the day may originate from photosynthetic activity (Evans, 2004). Typically, photosynthesis is a major source of oxygen for plants and rhizosphere in submerged species (Jackson and Armstrong, 1999). Submergence of photosynthetically active organs hinders the immediate supply of photosynthetically generated oxygen to the roots (Armstrong et al., 2019), as well as significant fluctuations in radial oxygen loss (ROL), which has a direct impact on the sediment oxidation (Waters et al., 1989; Pedersen et al., 1995, 2017). Aerenchyma acts as a conduit for oxygen in the root system, which is critical for wetland plants to survive in anoxic conditions (Armstrong et al., 1991). Through aerenchyma, oxygen needed by wetland plants can be transported from the above-ground plant parts to the rhizosphere of the submerged roots. Numerous wetland plants' roots contain a barrier that prevents oxygen from diffusing into the basal zones, thereby increasing longitudinal oxygen diffusion along the aerenchyma toward the root tips (Armstrong et al., 2000; Colmer, 2003), and ensuring oxygenation in the aerobic zone surrounding the growing tips (Striker et al., 2007). It is now widely accepted that the aerenchyma can act as ecological engineers by conferring the capacity to tolerate soil saturation (Jones et al., 1994; Booth and Loheide, 2010). Above all, fine root traits, specifically the aerenchyma, can be used to evaluate the wetland plants' functional characteristics to adapt to flooding stress (Purcell et al., 2019). However, from the eco-hydrological modeling perspective, the contribution of aerenchyma was not sufficiently considered.

To date, the effect of hydrology and soil physics on plant physiological responses to flooding has been investigated most extensively under controlled experimental conditions (DeLaune et al., 1990; Casanova and Brock, 2000; Hough-Snee et al., 2015; Kirwan and Guntenspergen, 2015; Byun et al., 2017; Zhang et al., 2019). While the effects of seasonal flooding on a few species under specific conditions have been determined in controlled experiments, the ability of wetlands plants to survive in natural settings was not extensively reported. It has been reported that plant communities with greater diversity in natural conditions are commonly more resistant to environmental disturbances and can respond positively to some mild flooding events than plants grown in monoculture or under controlled conditions (Reich et al., 2001; Isbell et al., 2015; Wright et al., 2015; Fischer et al., 2016; Cesarz et al., 2017). The majority of field studies on the interactions between abiotic factors and plant physiological responses have been conducted in salt marshes with low species diversity (Pezeshki et al., 1987; Pezeshki, 1998; Abou Jaoudé et al., 2012; Watson et al., 2015; Yan et al., 2018). Few model studies on the relationships between abiotic features and plant physiological responses have been conducted in natural inland seasonal flooding wetlands, but little is known about the root oxygen respiration rate (RORR) and aerenchyma functioning of typical wetland plants (Zhou et al., 2016; Pezeshki et al., 2018). Furthermore, there is still a need for a systematic method to link field experiments and eco-hydrological modeling to improve the parameterization of the physiological responses of typical wetland plant species to natural flooding events. Understanding the plant physiological responses enables us to gain insight into the functional characteristics of seasonal wetland environments. This may be especially important for natural floodplain wetlands, where the social and ecological importance is extremely high, while being seriously affected by drainage and reclamation with an estimated 95 km^2/year loss globally (Coleman et al., 2008).

This study aims to bridge the above-mentioned research gap by deploying a process-based eco-hydrological model and *in-situ* field experiments, applied to a natural floodplain wetland located in northeastern Heilongjiang Province, China. A site-scale eco-hydrological experiment was conducted in No.139 Monitoring Transect (EMT-139) of Honghe National Nature Reserve (HNNR) to compare the response patterns of two typical wetland plants to a natural flooding process. The LNPRs of flood-tolerant meadow species *Deyeuxia angustifolia* (Kom.) Y. L. Chang (MeS) and invading shrub species *Salix rosmarinifolia* Linn. var. *brachypoda* (Trautv.et Mey.) Y.L. Chou (ShS) were monitored in relations to the flooding regimes, root-zone soil moisture content (RZ-SWC), soil temperature (ST), and soil physio-chemical variables. Furthermore, a process-based eco-hydrological model specifically for calculating RORR was proposed for simulating plant physiological responses to natural flooding events. The following three hypotheses were tested: 1. The MeS with a preference for wet habitats has a competitive advantage over first-year invading ShS during flooding events; 2. The RORR is strongly correlated with the LNPR of the two plant types, particularly under flooding conditions during the growing

season; and 3. The aerenchyma sub-model may improve the eco-hydrological model's performance in accurately capturing the physiological dynamics of the plants in responses to natural flooding events.

MATERIALS AND METHODS

Study Area

The Sanjiang Plain is a cool temperate continental climate region with the most extensive and concentrated aquatic habitats in China, including freshwater marshes, marshy meadows, shrubs, forests, etc. (Zhou et al., 2009; Niu et al., 2012). The HNNR is located northeast of the Sanjiang Plain in Heilongjiang Province (47°42′18″–47°52′00″ N, 133°34′38″ –133°46′29″ E). The HNNR is designated as a Ramsar Wetland of International Importance (Gardner and Davidson, 2011). It is well-known for the Sanjiang Plain's "unique gene pool of wildlife" (Zhou et al., 2013). This wetland is 251 square kilometers in size. The annual precipitation averages 579.3 millimeters, while annual evaporation averages 1,166 mm. Between July and September, approximately 50–70% of the precipitation occurs. Each year, for more than 5 months, the soils freeze to depths of 160–180 cm (Li et al., 2011). Seasonal flooding is prevalent in the EMT-139 (**Figure 1**), resulting in a varying hydrological gradient that is either fully saturated, seasonally saturated, or unsaturated. In the EMT-139, two typical wetland plant types, the MeS and ShS, were compared and analyzed. The MeS is widespread wetland plant species in the Sanjiang Plain. It can survive and thrive under a variety of soil and water conditions. The MeS usually sparsely covered with shrubs, maintaining an open character. The ShS is also native plant community to certain marshy areas in the Sanjiang Plain and is well-adapted to dry soil conditions. However, when moisture levels in the upper soil layers are low due to insufficient rainfall and flooding, the local habitat becomes ideal for the ShS, allowing it to expand extensively. In the EMT-139, growing season in the year 2017 was marked by the invasion of the ShS over MeS.

Eco-Hydrological Modeling Framework

The eco-hydrological model building process is depicted in **Figure 2**. To begin, we simulated the root zone soil water content (RZ-SWC) of the MeS and ShS in the variably-saturated soil column. By comparing the soil water retention curve, the RZ-SWC, and the moisture at which capillary bonds rupture, the effective soil layers for the main growing root tips were identified. The optimal soil layer for the MeS root growth was found to be between 10 and 20 cm (Zhang et al., 2015), whereas the optimal soil layer for the ShS was between 30 and 40 cm (Blume-Werry et al., 2019). The second stage involved calculating the oxygen concentration in bulk soil at the macroscale using the simulated RZ-SWC from step 1 (Cook, 1995; Bartholomeus et al., 2008). The third step was to calculate oxygen concentration at the outer

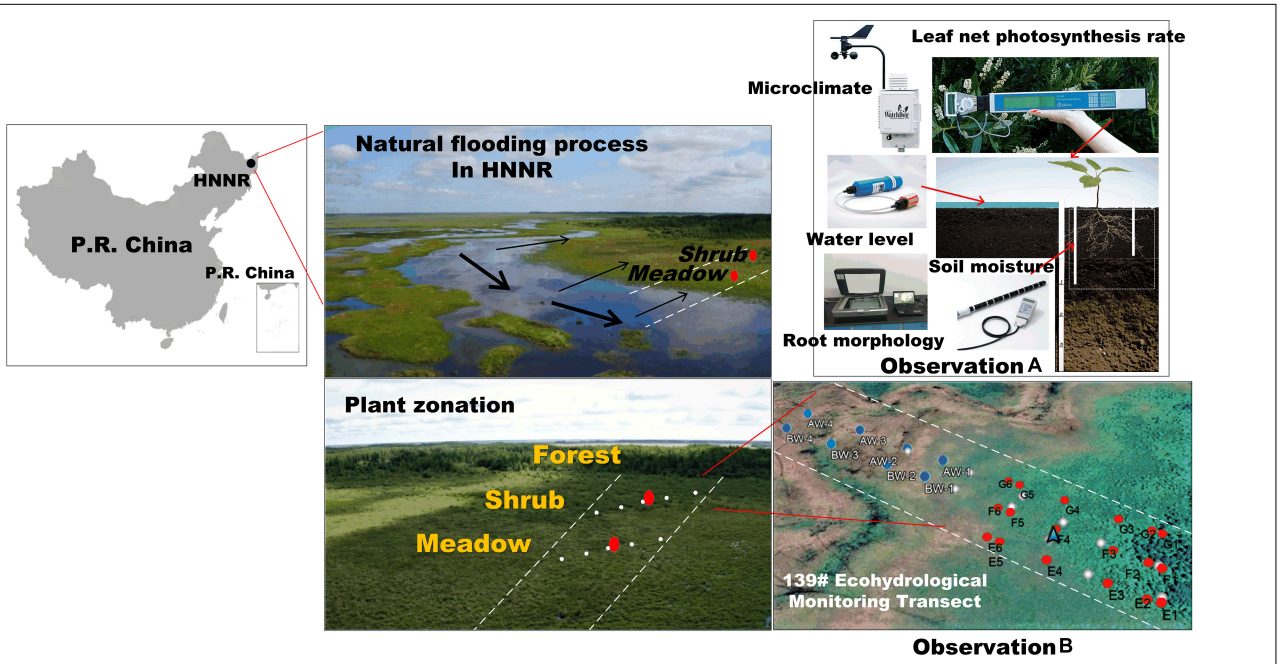

FIGURE 1 | Eco-hydrological experiments in an eco-hydrological monitoring transect (EMT-139) along a seasonal river in the HNNR in Heilongjiang Province, China. Observation B depicts the experimental transects established in the year 2011 (Li et al., 2011). *In-situ* eco-hydrological monitoring experiments were conducted continuously along this transect between the year 2011 and 2020. The observation matrix (red dots) covered the multi-layers' root-zone soil water contents (RZ-SWCs) at the transitional zone, whereas the observation matrix (blue dots) represented the *in-situ* monitoring of the surface water level (SWL) of the seasonal Nongjiang River; The observation matrix (white dot) represented the check observations of the RZ-SWCs. Observation A illustrates the detailed eco-hydrological monitoring of each PFT on a site by site basis, which included *in-situ* monitoring of the leaf net photosynthesis rate (LNPR), RZ-SWC, SWL, and soil temperature (ST), as well as root and soil sampling of the meadow species (MeS) and shrub species (ShS).

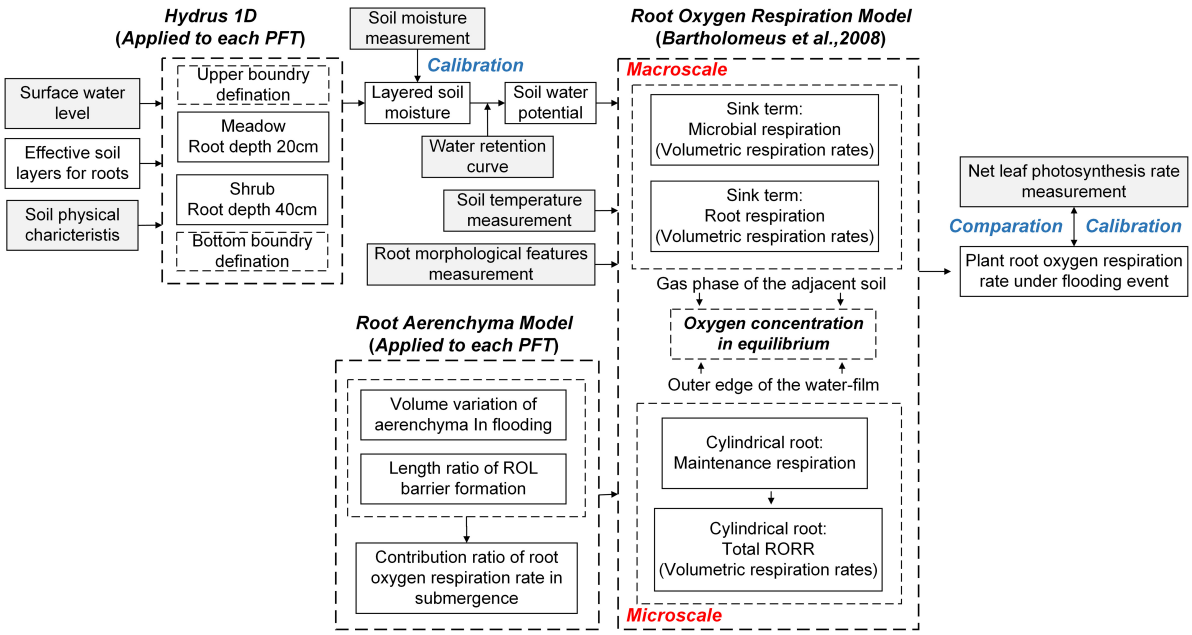

FIGURE 2 | The model framework of the present study (building process of the eco-hydrological model). Gray-colored boxes underlines the data from field experiments.

edge of the water-film adjacent to the root from macroscale to microscale. Following step 3, a new root aerenchyma model was developed in step 4 to account for the microscale physiological function of aerenchyma during flooding events. Finally, based on Bartholomeus et al. (2008), we simulated the RORR-MeS and RORR-ShS at the microscale, evaluated the biotic and abiotic parameter sensitivities of the new model, and investigated the link between the RORR and LNPR.

Root Zone Soil Water Content

The RZ-SWCs of the MeS and ShS were quantitatively simulated by solving the Richards Equation in the variably-saturated wetland soil environment using the USDA Salinity Laboratory's HYDRUS1D software (Simunek et al., 2005). The top 10 cm soil layer was defined as the organic surface layer (Bai et al., 2005), which contains finely divided organic matter and dead roots. This layer is in direct contact with the hydro-meteorological conditions at the surface and mineral soil layers beneath. Thus, in the parameterization scenario, the upper boundary condition was set to the variable pressure head, while the bottom layer was set to the variable flux. The model domain was extended to a depth of one meter, and a simulation period from 24 June to 1 October 2017 with a time step of 1 day.

Root Oxygen Respiration Rate

At the macroscale, microbial and root respiration were defined as two separate sink terms in the soil columns. Each term was defined using a reference value at $z = 0$ ($R_{microbial\_z0}$ and R_{root_z0} (kg O^2 m^{-3} d^{-1} soil) and an exponential shape factor [$Z_{microbial}$ and Z_{root} (m)] (Cook, 1995; Bartholomeus et al., 2008). The equilibrium was assumed to be achieved at soil depth z (m) in wetland soils. The oxygen concentration $C_{bulksoil}$ in the gas phase at soil depth z was calculated as follows under both flooding and non-flooding conditions:

$$C_{bulksoil} = C_{(atm,fw)} - \left(Z^2_{microbial} \cdot \frac{R_{microbial\_z0}}{D_{soil}}\right)\left(1 - exp\left(-\frac{z}{Z_{microbial}}\right)\right) - \left(Z^2_{root} \cdot \frac{R_{root\_z0}}{D_{soil}}\right)\left(1 - exp\left(-\frac{z}{Z_{root}}\right)\right) \quad (1)$$

where $C_{(atm,fw)}$ is used to express the oxygen concentration (kg O^2 m^{-3} d^{-1} soil) in the atmosphere or flooding water, respectively. D_{soil} is the mean diffusivity of the soil (m^2 d^{-1}).

Microbial respiration varies due to soil water dynamics and soil temperature, therefore the volumetric microbial respiration rates $R_{microbial}$ (kg O_2 m^{-3} soil d^{-1}) in the bulk soil were expressed as:

$$R_{microbial} = R_{microbial\_z0} exp\left(-z/Z_{microbial}\right) \quad (2)$$

$$R_{microbial\_z0} = \mu \beta f_{\varphi} Q_{10\_microbial}^{(T_{soil} - T_{ref})/10} \quad (3)$$

where μ is organic carbon content of the soil (kg C m^{-3} soil), β is vegetation dependent respiration rate (kg O^2 kg^{-1} C d^{-1}), f_{φ} is the factor which represents the reduction of microbial activity due to soil moisture availability (Probert et al., 1998; Arora, 2003), T_{soil} is soil temperature (K) at certain depth (m), T_{ref} is reference temperature (K), $Q_{10\_microbial}$ is relative increase in microbial respiration.

The oxygen concentration at the outer edge of the water-film C_{wfedge} and the gas phase of the adjacent soil $C_{bulksoil}$ were considered to be in equilibrium, thus the macro-to-microscale transformation was as follows:

$$C_{bulksoil} = C_{wfedge}/\alpha_B \quad (4)$$

where α_B is the Bunsen solubility coefficient for oxygen (m^3 gas m^{-3} liquid) (Weiss, 1970).

At the microscale, the total water-film respiration rate $r_{waterfilm}$ of a cylindrical root was calculated as follows:

$$r_{waterfilm} = r_{waterfilm\_z0} exp(-z/Z_{microbial}) \quad (5)$$

$$r_{waterfilm\_z0} = 0.5(\mu A)\beta Q_{10\_microbial}^{(T_{soil}-T_{ref})/10} \quad (6)$$

where T_{soil} (°C) is the soil temperature at certain soil depth, A is the area of the water-film cross-section (m^2). The cylindrical root oxygen respiration rate (μmol m^{-2} s^{-1}) at the micro-scale were calculated (Lemon and Wiegand, 1962; De Willigen and Van Noordwijk, 1984; Bartholomeus et al., 2008) as follows:

$$r_{cylin\_root} = \frac{4\pi C_{wfedge} D_{waterfilm} - r_{waterfilm} + 2r_{waterfilm} log_{10}^{(1+R_2)} M^{\frac{R_1}{R_2}}}{1 + R_1 log_{10}^{(1+R^2)}} \quad (7)$$

where $M = (1R_2)^2 (2R_2)$, $R_1 = D_{root}/D_{waterfilm}$, $R_2 = WFT_{waterfilm}/RS_{root}$. $WFT_{waterfilm}$ is the water-film thickness (m), RS_{root} is the root radius (m) of the cylindrical root, $D_{waterfilm}$ is the diffusivity of the water-film (m^2 d^{-1}). For a detailed definition and description of the equations and parameters used in the RORR simulation, please refer to Bartholomeus et al. (2008).

Root Aerenchyma

Upon soil waterlogging, oxygen transports through the gas conducting tissue (inducible and secondary aerenchyma) can occur *via* simple diffusion or pressure flow (Armstrong et al., 2000; Evans, 2004). In aerenchyma, oxygen is transported *via* diffusion through the pipe to the root tips. In this model, the cylindrical root's aerenchyma pipe structure was treated as a circular truncated cone (CTC) by summing up the volumes of all the individual aerenchyma pipes. The oxygen concentration in the aerenchyma is maintained at a constant level. Increased aerenchyma volume ratio during soil emergence in flooding-tolerant meadow and first-year invading shrub could, above all, correspond to increased oxygen respiration rates per unit time.

According to Montagnoli et al. (2019), volume variation of aerenchyma $P_{aerenchyma\_(MeS,\ ShS)}$ of both plant types under non-flooding and flooding conditions can be expressed as follows:

$$P_{aerenchyma\_(MeS,ShS)} = \frac{V_F}{V_{NF}} = \frac{R_F^2 + R_F \cdot r_F + r_F^2}{R_{NF}^2 + R_{NF} \cdot r_{NF} + r_{NF}^2} \quad (8)$$

where, V_F and V_{NF} are the aerenchyma volumes (m^3) under flooding and non-flooding conditions, respectively. R_F and r_F indicate lower and upper bases of the CTC under flooding conditions (m), while R_{NF} and r_{NF} are the lower and upper bases of the CTC under non-flooding conditions (m). $P_{aerenchyma}$ was determined using data from greenhouse experiments (Maricle and Lee, 2002), in which the amount of aerenchyma along the lengths of roots was determined under flooding and non-flooding conditions.

Following submergence, an out cortex ROL barrier with a length ratio $\frac{Barrier_{(MeS,\ ShS)}}{Length_{(MeS,\ ShS)}}$ formed accordingly. Therefore, available oxygen to cultivate root tips was formulated at an update ratio $R_{(MeS,\ ShS)}$:

$$R_{(MeS,ShS)} = \frac{Length_{(MeS,ShS)}}{Length_{(MeS,ShS)} - Barrier_{(MeS,ShS)}} \quad (9)$$

However, in comparison with the MeS, the ROL barrier in roots of ShS was inadequate. This resulted in the insufficient oxygen transport to root tips during flooding, thereby poor oxygenation of the rhizosphere zone (Blom, 1999). According to ROL experiment results in Watanabe et al. (2017) and Yamauchi et al. (2018), the $\frac{Barrier_{(MeS,ShS)}}{Length_{(MeS,ShS)}}$ after flooding were set to 0.625, 0.325 in the present study, respectively.

All in all, the contribution rate $CAR_{Flooding}$ of both aerenchyma and the ROL on the RORRs during flooding can be formulated as follows:

$$CAR_{Flooding\_MeS} = P_{aerenchyma\_MeS} Q_{10\_aerenchyma\_MeS}^{(T_{soil\_MeS}-T_{ref})/10} exp(R_{MeS}) \quad (10)$$

$$CAR_{Flooding\_ShS} = P_{aerenchyma\_ShS} Q_{10\_aerenchyma\_ShS}^{(T_{soil\_ShS}-T_{ref})/10} \quad (11)$$

where, $Q_{10\_aerenchyma\_(MeS,ShS)}$ is the rate of relative increase in aerenchyma activity intensity with a temperature increase of 10°C, with values of 1.1 and 1.2 for the MeS and ShS, respectively. In the current study, this indicates the increased respiration intensity induced due to increases in soil and rhizosphere temperature.

Eco-Hydrological Experiments in the No.139 Monitoring Transect

The shrub encroachment in the year 2017 was driven by the colonization of *Salix rosmarinifolia* Linn. var. *brachypoda* (Trautv.et Mey.) Y.L. Chou into former meadow areas. Current study categorized *Deyeuxia angustifolia* (Kom.) Y. L. Chang and *Salix rosmarinifolia* Linn. var. *brachypoda* (Trautv.et Mey.) Y.L.Chou into two plant functional types (PFTs): flood-tolerant meadow and first-year invading shrub. This classification system can be used to evaluate the physiological response of two representative plant types in the EMT-139 to seasonal flooding events. For each PFT, 10 samples were randomly selected that appeared to be healthy in appearance and stood approximately 60 cm high for the MeS and 130 cm high for the ShS. For each sample, the LNPR was measured daily with the CI-340 Handheld

Photosynthesis System (CID Bio-Science, Inc., United States) during the early to mid-morning hours. Young leaves of each sample were placed into the leaf chamber and the measurement results were recorded when the screen displayed a stable value, which typically took 2–5 min. On 16 September 2017, four individual plants of each PFT were harvested (above- and below-ground). We used the data collected during this period because the plant's maximum biomass occurs during this vegetative stage. The entire root systems were carefully harvested and rinsed with tap water, and the fresh mass was recorded. The root systems were oven-dried for 48 h at 65°C and then weighed. Sections of the fresh root system were carefully separated from each species and scanned immediately at a resolution of 600 dpi with a flat-bed transparent lighting system using an Expression 10000 XL 3.49 scanner (Epson Telford Ltd., United Kingdom). WinRHIZO Pro2012b software (Regent Instruments, Inc., Canada) was used to analyze the root images for the average diameter (mm), specific root length (SRL, m g^{-1}), and specific root area (SRA, cm^3 g^{-1}), etc. The root total organic carbon (TOC, g kg^{-1}) and total nitrogen (TN) (ROC, g kg^{-1}) were then measured with a Nitrogen analyzer multi N/C 2100 (Analytik Jena AG, Germany) using a dry combustion method.

Hydrological experiments in the EMT-139 measured the basic hydrological conditions for plants across the growing season. Simultaneous measurements of precipitation, surface water, and soil water content were made. It contains surface water level (SWL) (m), multi-layer RZ-SWCs (volume moisture content, cm^3/cm^3), micrometeorological variables, and determination of soil water retention curve from 24 June 2017 to 1 November 2017. Odyssey capacitance water level loggers (Dataflow Systems Ltd., New Zealand) were installed in eight PVC pipes (AW1-AW4, BW1- BW4) to monitor the actual SWL along the Nongjiang River's cross section in the EMT-139 (**Figure 1**). The RZ-SWCs were measured using a Delta-T Devices PR2 profile probe (Delta-T Devices Ltd., United Kingdom). The instrument was one meter in length and was placed into thin wall-mounted tubes with sensor pairs at 10, 20, 30, 40, 60, and 100 cm depth. There were 24 PR2 sites in the EMT-139 and the RZ-SWCs were measured manually. The WatchDog 2000 Series Weather Station (Spectrum Technologies, Inc., United States) was installed in the central part of the EMT-139. Since June 2017, microclimate data series had been recorded every 6 h, which contained precipitation, wind speed, air temperature, air humidity, solar radiation, etc. Water retention curve is a critical soil hydraulic characteristic that must be considered when solving soil water flow equations (Zeng et al., 2011). The water potential of soil samples was determined using the WP4C Soil Water Potential Lab Instrumentation (METER Group, Inc., United States). By using RETC software (Salinity Laboratory, USDA), the Van Genuchten equation (Van Genuchten, 1980) was fitted to the measured RZ-SWCs and soil matric potential data (**Table 1**).

Data Analyses

The simulated RZ-SWC values by HYDRUS1D were compared to those measured *in-situ* in EMT-139. The Relative Root Mean Square Error (RRMSE) (Zeng, 2013) and coefficient of determination (R^2) were used to evaluate the simulation

TABLE 1 | Measured soil physical and chemical properties and root morphology within the observation sites in the EMT-139.

Plant type	Soil depth	Soil hydraulic parameters[a]					Soil chemical properties[b]			Biomass (dry weight)		Root morphology[c]	
EMT-139	(cm)	θ_s (cm^3 cm^{-3})	θ_r (cm^3 cm^{-3})	α (cm^{-1})	N (−)	K_s (mm day^{-1})	TN (g kg^{-1})	TC (g kg^{-1})	SOC (g kg^{-1})	Aboveground (g)	Root (g)	SRL (m g^{-1})	SRA (cm^3g^1)
MeS	0–10	0.76	0.13	0.04	1.27	3181.60	13.43	128.43	221.42	1.07	0.09	28.03	362.34
	10–20	0.54	0.10	0.02	1.34	257.60	5.15	15.78	63.57				
	20–30	0.49	0.10	0.02	1.30	103.80	3.31	8.86	21.24				
	30–50	0.46	0.10	0.02	1.28	62.50	2.25	3.65	10.78				
	50–70	0.47	0.10	0.02	1.24	77.70	2.08	2.53	4.35				
	70—-100	0.46	0.10	0.02	1.21	63.40	1.67	1.58	2.72				
ShS	0–10	0.68	0.12	0.02	1.31	1708.90	6.31	71.05	122.48	7.57	3.20	3.63	49.24
	10–20	0.58	0.11	0.02	1.33	565.90	1.97	14.25	38.42				
	20–30	0.50	0.10	0.01	1.39	151.20	2.20	3.62	24.57				
	30–50	0.44	0.09	0.01	1.32	44.10	1.97	4.04	6.96				
	50–70	0.44	0.10	0.02	1.21	49.80	2.01	4.02	6.93				
	70–100	0.45	0.10	0.02	1.23	60.40	2.33	4.60	7.93				

[a]*Soil hydraulic parameters of Van Genuchten equation were fitted using RETC software.*
[b]*Values shown averaged over soil samples in EMT-139.*
[c]*Values shown averaged over root samples in EMT-139.*

performance. The data analyses were done by using the OriginPro (OriginLab Corporation, United States).

$$RRMSE = \frac{\sqrt{\sum_{i=1}^{N_M}(M_i - S_i)^2 / N_M}}{Max\left(M_1, M_2, \ldots\ldots, M_{N_M}\right) - Min\left(M_1, M_2, \ldots\ldots, M_{N_M}\right)} \quad (12)$$

$$R^2 = 1 - \frac{\sum_{i=0}^{N_M}(M_i - S_i)^2}{\sum_{i=0}^{N_M}\left(M_i - \overline{M}\right)^2} \quad (13)$$

where N_M is the number of the soil moisture measurements; M_i and C_i are the value of soil moisture measurements and HYDRUS1D simulations; $Max\left(M_1,\ M_2, \ldots\ldots, M_{N_M}\right)$ and $Min\left(M_1,\ M_2, \ldots\ldots, M_{N_M}\right)$ are the maximum and minimum values of the soil misture measurements, respectively; $\overline{M}$ is the mean of the soil moisture measurements. The *RRMSE* and R^2 are dimensionless. The lower the *RRMSE*, the closer the simulated values approach the observed values, while higher R^2 values indicates better agreement.

The RORRs of the MeS and ShS were simulated and compared to the measured LNPRs in the EMT-139. The performance of correlations was evaluated by the Pearson Correlation Coefficient (PCC) and coefficient of determination (R^2).

$$PCC = 1 - \frac{\sum_{i=0}^{N_M}\left(SR_i - \overline{SR}\right)\left(ML_i - \overline{ML}\right)}{\sqrt{\sum_{i=0}^{N_M}\left(SR_i - \overline{SR}\right)^2}\sqrt{\sum_{i=0}^{N_M}\left(ML_i - \overline{ML}\right)^2}} \quad (14)$$

where SR_i and ML_i are the value of the RORR simulations and LNPR measurements; $\overline{SR}$ and $\overline{ML}$ are the mean of the RORR simulations and LNPR measurements. The PCC value range from −1 to +1. A value of +1 indicates total positive linear correlation, 0 indicates that there is no linear correlation, and −1 is total negative linear correlation.

RESULTS

Soil Properties and Morphological Characteristics of the Roots

The physio-chemical properties of the soil profile, the biomass and root morphological characteristics of the two plant types observed in the EMT-139 are shown in **Table 1**. The vertical permeability of multi-layer soil profiles was found to vary due to layered deposition or biological activity-induced soil gradient characteristics. Additionally, as a key soil-water characteristic, the saturated hydraulic conductivity (Ks) of the 0–10 cm layer of the MeS is much greater than the ShS', indicating a higher water flow rate, and a more efficient partitioning of rainfall and surface water into soil water storage. Moreover, the saturated hydraulic conductivity, the concentrations of total nitrogen, total carbon, and organic carbon of both soils were quite low below 40 cm depth, showing that these dense, impervious, and low-nutrient layers isolated the groundwater interaction and were unfavorable for root system penetration and growth. Furthermore, despite the lower above- and below-ground biomass, the MeS' specific root length (SRL) and specific root area (SRA) were approximately eight times larger than the ShS', reflecting a stronger capacity for adapting to environmental changes throughout the growing season.

Simulation Results of the Root-Zone Soil Moisture Content

Figure 3 depicted the observed and simulated RZ-SWCs of the MeS and ShS. The simulation results were generally in good agreement with the observations. The RRMSE values of RZ-SWC at 20 cm depth in MeS and 40 cm in ShS were 0.229 and 0.117, while the R^2 values were 0.650 and 0.906, respectively. The simulated RZ-SWCs in the MeS and ShS could follow the general trend of the observations over the study period. Better agreements with the observations were achieved in the ShS. Exceptions were noted during the flooding periods and thereafter, when the simulated results of MeS were a bit higher than the observed recession curves, while the ShS' were slightly lower. The upper boundary condition specifications may partially explain the overestimated simulated results. It was assumed that surface water directly infiltrated into the underlying mineral profiles, disregarding any horizontal runoff processes of this layer, therefore promoting soil columns with higher water input and consequently increasing the simulated RZ-SWC of MeS; Underestimated ShS' may had been influenced by the flow and redistribution of water in "horizontal soil columns" of varying textures. In the field condition, a fairly obvious leaching layer was observed at approximately 40 cm depth in the EMT-139 along the riverside, which may also contributed to the underestimation.

Simulation Results of the Root Oxygen Respiration Rate

Notably, simulated RORRs of the MeS and ShS were generally in good agreement with the measured LNPRs (**Figure 4**). Better correlations were achieved in the MeS. The MeS and ShS had PCC values of 0.847 and 0.850, respectively, while R^2 value were 0.717 and 0.722. It is noteworthy that the RORR simulation results for the MeS and ShS could almost follow the general trend of the LNPR observation values over the study period. As illustrated in **Figures 4A,B**, surface flooding from 31th July 2017 immediately suppressed the RORRs and LNPRs in both plant types. A noticeable trend was the sharp decline following the occurrence of surface water flooding. Interestingly, the RORR-MeS increased from a trough value 0.22 μmol m^{-2} s^{-1} within 1–2 days and recovered to nearly normal level within approximately 10 days. However, for the ShS, the RORR value dropped dramatically shortly after the surface flooding, and remained nearly constant at an average value of 0.30 μmol m^{-2} s^{-1} onwards, which indicated a deadly flooding impact on the root functioning of the ShS. This demonstrated an advantageous effect of flooding on shrub expansion restriction (Myers-Smith et al., 2015).

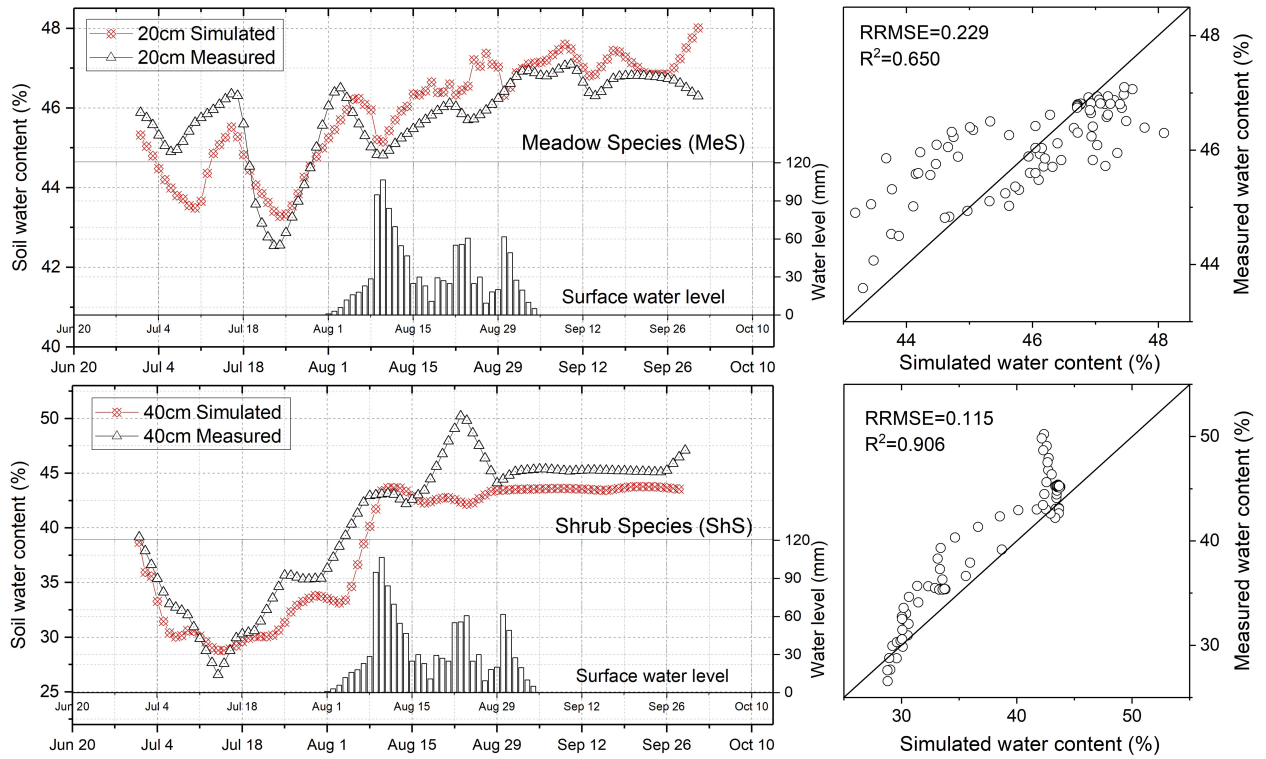

FIGURE 3 | Observed and simulated RZ-SWCs of the MeS and ShS at certain soil depths. Scatter tracks illustrate the difference between the observed and simulated RZ-SWCs by displaying the mean radically root square error (RRMSE) and the determination coefficient (R^2).

Influence of the Aerenchyma Sub-Model to the Root Oxygen Respiration Rate Simulation Results

The effect of the aerenchyma sub-model on simulation results of the RORR for the MeS and ShS was investigated. As indicated in **Figure 5**, the simulated values of the RORR-MeS and RORR-ShS during periods of surface flooding were considerably underestimated (18.96 and 16.37%, respectively) without the aerenchyma sub-model. This emphasized the critical role of the aerenchyma's physiological function under flooding stress. Developing appropriate aerenchyma models would assist in quantifying the dynamics of plant physiological responses to flooding events.

DISCUSSION

The Performance of Current Eco-Hydrological Model

In this study, we simulated the physiological responses of typical wetland plants to natural flooding events by using a process-based eco-hydrological model. Additionally, a new root aerenchyma sub-model was developed and incorporated into the above-mentioned model. This sub-model contained key processes of root oxygen diffusion and ROL during soil submergence. The aerenchyma model improved the precision of root oxygen respiration rate simulation, thereby would enhance the understanding of the structure and function of aerenchyma in wetland plants during seasonal flooding events. Furthermore, soil moisture was successfully simulated in variably saturated wetland conditions under the assumption that the wetland surface litter layer was specified as a 10 cm top soil layer. When surface flooding water was present, the simulation results closely matched the observations. Overall, we improved the model reliability in representing the eco-hydrological processes and parameterization of abiotic and biotic factors, which were both considered concurrently when simulating the RORR-MeS and RORR-ShS. Notably, we observed an exception that the RORR-ShS value did not vary significantly in comparison to the LNPR-ShS value before the rainy season. We hypothesize that this could be due to the ShS' unique physiological characteristics, which enabled it to maintain a steady RORR during dry seasons, thereby establish stable whole-plant source-sink relationships in this stage (Pregitzer et al., 2000).

Relationship of the Root Oxygen Respiration Rate and Leaf Net Photosynthesis Rate

The present study confirmed previous findings that oxygen diffusing to the roots and rhizosphere during the day may be a result of photosynthetic activities (Caffrey and Kemp, 1991; Evans, 2004). Moreover, in submerged species, photosynthesis

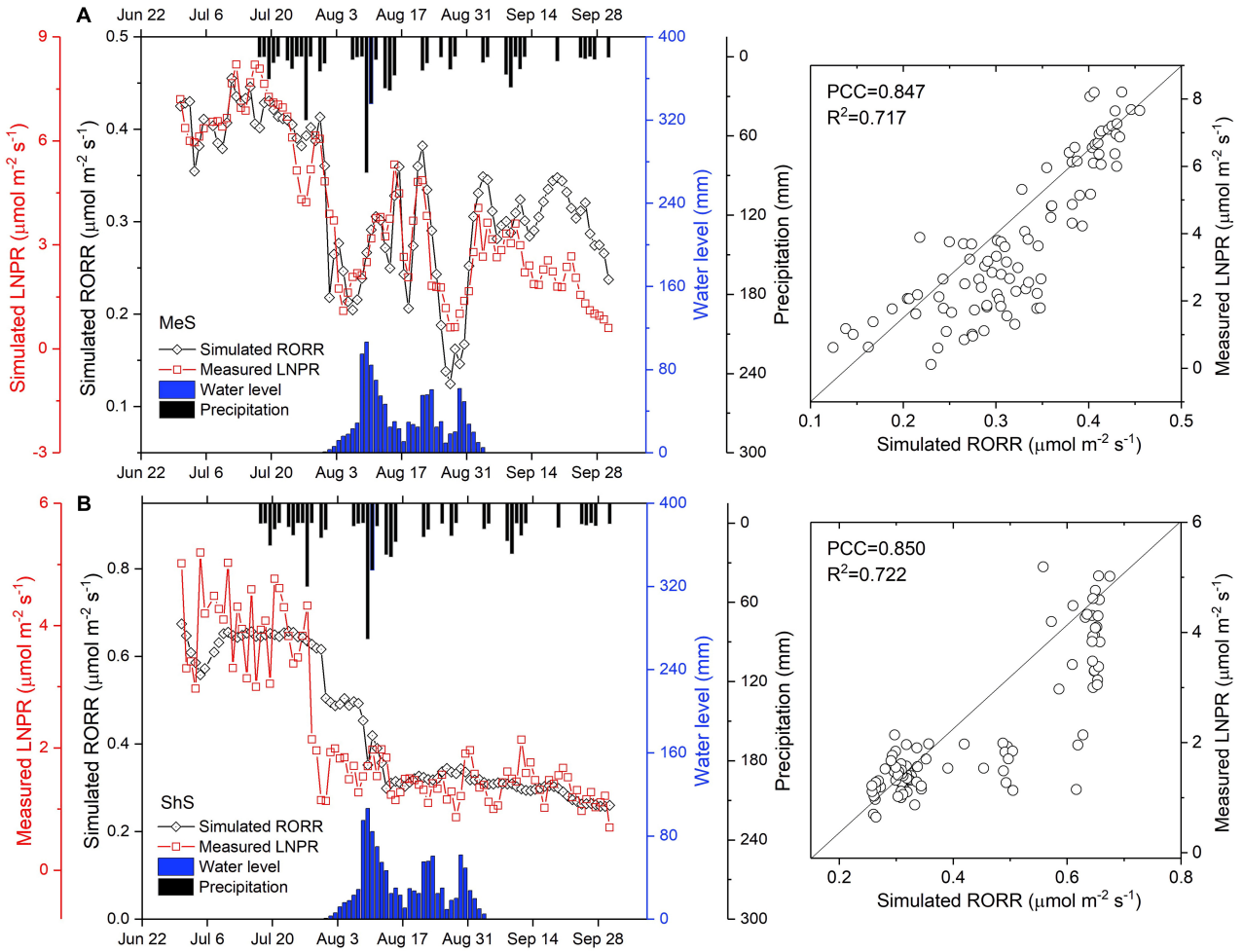

FIGURE 4 | Simulated root oxygen respiration rate (RORR) and measured leaf net photosynthesis rate (LNPR) of the MeS **(A)** and ShS **(B)** under the influence of rainfall and surface water level. Scatter tracks demonstrate the relationship between the observed and simulated values of the MeS and ShS by displaying Pearson Correlations Coefficients (PCC) and the determination coefficient (R^2).

was a significant source of oxygen for the fine root and rhizosphere (Jackson and Armstrong, 1999). Diurnal changes in root respiration strongly correlated with rates of net photosynthesis (Lai et al., 2016). As illustrated in **Figures 4A,B**, during the initial stage of seasonal flooding, when the rhizosphere was hypoxic, both leaf photosynthetic capacity and root oxygen respiration rate of the Mes and ShS were significantly affected. However, the MeS with a preference for wet microhabitats had a competitive advantage over first-year invading ShS under flooding stress, which was consistent with previous researches (Jung et al., 2008; Gattringer et al., 2017, 2018). Flooding had a detrimental effect on the ShS due to the physiological dysfunctions caused by soil anaerobiosis (Kozlowski, 2002). To summarize, the RORRs correlated positively with the LNPRs in both plant types during flooding events. However, it should be noted that, from 31st August onwards, there was a noticeable recovery (averaged 0.32 μmol m^{-2} s^{-1}) of the RORR-MeS, which outnumbered the LNPR-MeS as a whole during this period. This may help explain, at least in part, why fine root production exceeded above-ground production. That is, as evidenced by measurement data from a variety of biomes, seasonal variation in root production cannot always be attributed to above-ground production (Abramoff and Finzi, 2015). Therefore, typical wetland plants may increase the level of RORR to prepare for the next life-cycle stage.

Influences of the Root-Zone Soil Moisture Content and Soil Temperature on the Root Oxygen Respiration Rate

Monte Carlo methods were used to evaluate the sensitivity of the RORR to root-zone soil water stress associated with the soil temperature (Hammersley, 2013). To begin, the RZ-SWC was randomly selected from normal distributions using the mean and standard deviation values from the HYDRUS1D simulation results. Then, the RORR-MeS and RORR-ShS were simultaneously simulated, with the inputs from the normalized RZ-SWC and ST. The RORR's sensitivity to RZ-SWC and ST was

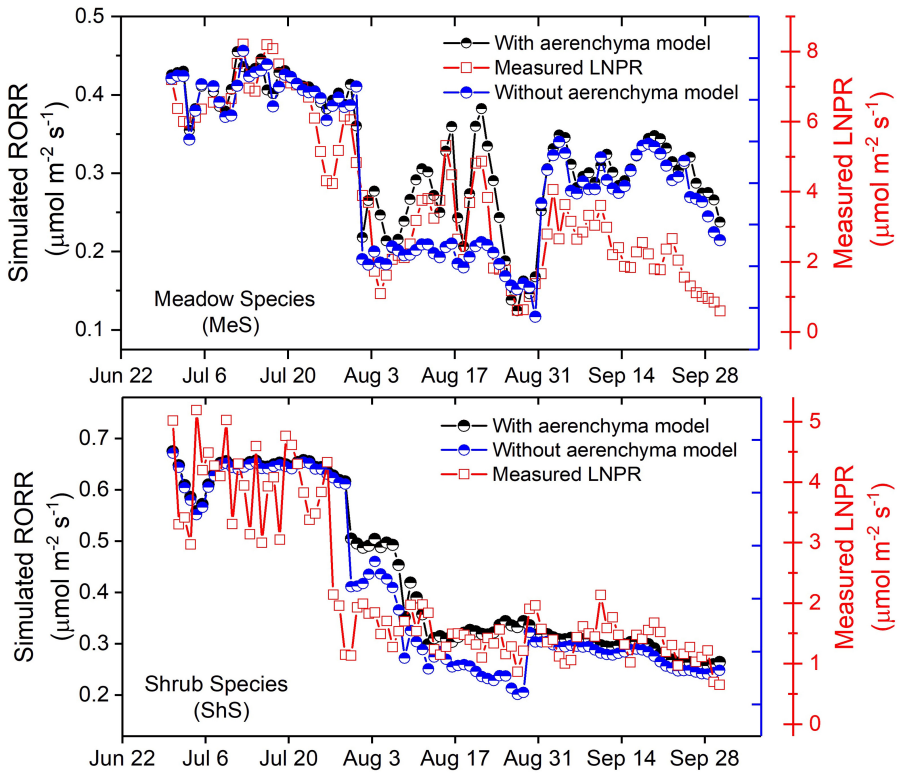

FIGURE 5 | Comparison of the RORR and LNPR simulation results of the MeS and ShS with and without the aerenchyma sub-model.

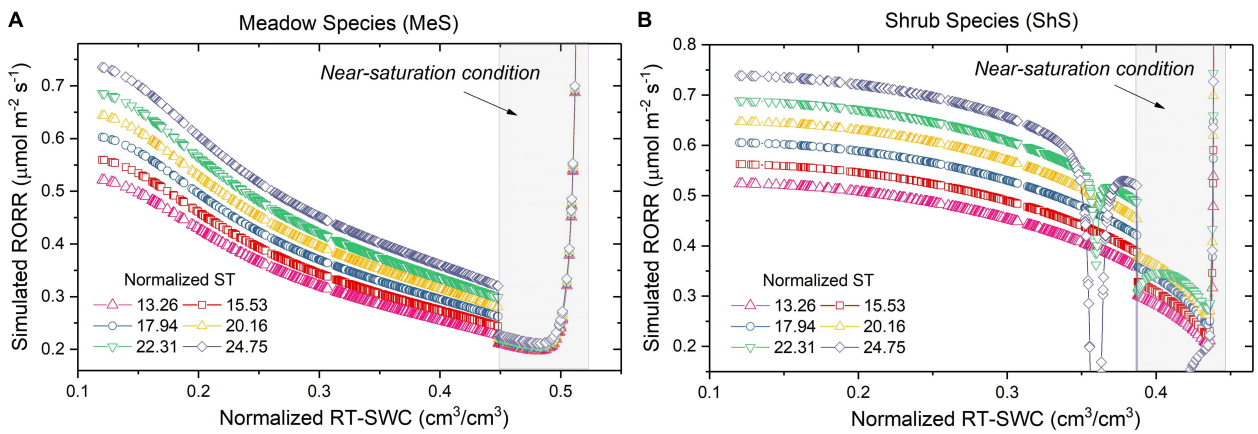

FIGURE 6 | Sensitivity of the RORRs to RZ-SWCs at various ST (ranging from 13.26 to 24.75°C) for the MeS **(A)** and ShS **(B)**. Gray areas indicates the near-saturation conditions.

then visualized by using linear regression methods. Sensitivity analysis reveals that the RZ-SWC had a ST-dependent effect as illustrated in **Figures 6A,B**. Interestingly, the RORR-MeS was more susceptible to ST fluctuations than the RORR-ShS under low RZ-SWC conditions. By contrast, the RORR-ShS (**Figure 6B**) was more sensitive to ST fluctuations than the RORR-MeS at the state of near saturation, with the RORR-MeS exhibited no apparent ST dependence (**Figure 6A**) at this stage. It is noted that RORR-ShS was more sensitive to the ST above approximately 20 °C, which resulted in a significant decrease in RORR-ShS values. In other words, the ST over 20 °C caused more RORR damage to the roots of the ShS than to the MeS'. Moreover, the RORR-MeS was more stable over a wider range of RZ-SWC values (upper limit: 0.53 cm^3/cm^3) than the RORR-ShS (upper limit: 0.44 cm^3/cm^3). Notably, the RORR-MeS could recover, at least to some extent, before the state of full saturation. This reflects a stronger capacity of the MeS adjusting the root oxygen respiration function under flooding conditions.

Above all, sensitivity analysis demonstrated that the RORR responses may differ according to plant types and stages in relations to the combined effects of temperature and soil saturation, as evidenced by Calleja-Cabrera et al. (2020). The MeS appeared to respond to the combined stresses more effectively by increasing oxygen partitioning to the roots, thereby promoting rhizosphere oxidation and fine root growth. When both stresses were present, in contrast to the MeS, the harmful effects were amplified for the ShS, because they were more intolerant to relatively high RZ-SWC and ST (Atkin et al., 2000).

Limitations of the Current Study

This study has two main limitations. The first limitation is the observational error in natural wetlands. The hydrological complexity of the seasonal flooding intensified the difficulty of *in-situ* multi-layered soil moisture measurement. This may partially resulted in not good agreement (with the RRMSE values 0.229, and the R^2 values 0.650) of the simulated RZ-SWC-MeS with the observations. Second, the current eco-hydrological model did not include all the key physiological processes to adapt to flooding stress. For example, flooding-induced adventitious roots (They contain aerenchyma cells as well) have been described for a number of Central European shrub species (Glenz et al., 2006), which can also maintain the root respiration *via* rapid oxygen absorption. Therefore, in order to more effectively simulate the physiological response to seasonal flooding events, the adventitious roots should be incorporated into the eco-hydrological model in the future.

CONCLUSION

A process-based eco-hydrological model for the physiological responses of typical wetland plant species to natural flooding events, has been developed and validated with the data from *in-situ* field measurements from a natural wetland in northeastern China. The new root aerenchyma sub-model was able to improve the precision of root oxygen respiration rate simulation. The results presented here show that we improved the model reliability in representing the eco-hydrological processes and parameterization of abiotic and biotic factors. The study also shows a strong correlation between the root oxygen respiration rate and the leaf net photosynthesis rate during natural flooding events. This would contribute to eco-hydrological modeling science with a new way of understanding the key processes in floodplain wetlands. This would also assist in more accurate assessments and predictions of vegetation dynamics for wetland management and restoration initiatives. Restoration of degraded or destroyed freshwater wetlands can be achieved by designing regulatory flooding processes that efficiently restore native flood-tolerant wetland vegetation and restrict woody plant invasion. This study will be expanded in the future to deal with the physiological responses at a larger spatio-temporal scale by developing a more comprehensive eco-hydrological model, thereby providing mathematical tools for exploring the spatio-temporal patterns of plant physiological responses in natural floodplain wetlands.

DATA AVAILABILITY STATEMENT

The original contributions presented in the study are included in the article/**Supplementary Material**, further inquiries can be directed to the corresponding author/s.

AUTHOR CONTRIBUTIONS

CL, YZ, ZS, and DZ conceived and designed the study. YZ, ZS, and DZ establish the context for field experiments and simulations. CL conducted experiments and simulations and wrote the manuscript. All authors contributed to developing the model and provided feedback on earlier drafts and approved the final version for submission.

FUNDING

This work was supported by grants from the National Natural Science Foundation of China (NSFC41671509).

ACKNOWLEDGMENTS

We would like to express our gratitude to the Sanjiang Experimental Station of Wetland Ecology, Northeast Institute of Geography and Agroecology, Chinese Academy of Sciences, for supporting the Eco-Hydrological Experiments in this study.

SUPPLEMENTARY MATERIAL

The Supplementary Material for this article can be found online at: https://www.frontiersin.org/articles/10.3389/fevo.2022.721244/full#supplementary-material

REFERENCES

Abou Jaoudé, R., de Dato, G., and De Angelis, P. (2012). Photosynthetic and wood anatomical responses of *Tamarixafricana* poiret to water level reduction after short-term fresh-and saline-water flooding. *Ecol. Res.* 27, 857–866. doi: 10.1007/s11284-012-0963-3

Abramoff, R. Z., and Finzi, A. C. (2015). Are above-and below-ground phenology in sync? *New Phytol.* 205, 1054–1061. doi: 10.1111/nph.13111

Armstrong, W., Beckett, P. M., Colmer, T. D., Setter, T. L., and Greenway, H. (2019). Tolerance of roots to low oxygen: 'Anoxic' cores, the phytoglobin-nitric oxide cycle, and energy or oxygen sensing. *J. Plant Physiol.* 239, 92–108. doi: 10.1016/j.jplph.2019.04.010

Armstrong, W., Brändle, R., and Jackson, M. B. (1994). Mechanisms of flood tolerance in plants. *Acta Bot. Neerl.* 43, 307–358. doi: 10.1111/j.1438-8677.1994.tb00756.x

Armstrong, W., Cousins, D., Armstrong, J., Turner, D., and Beckett, P. (2000). Oxygen distribution in wetland plant roots and permeability barriers to gas-exchange with the rhizosphere: a microelectrode and modelling study with phragmites australis. *Ann. Bot.* 86, 687–703. doi: 10.1006/anbo.2000.1236

Armstrong, W., Justin, S., Beckett, P., and Lythe, S. (1991). Root adaptation to soil waterlogging. *Aquat. Bot.* 39, 57–73. doi: 10.1016/0304-3770(91)90022-w

Arora, V. K. (2003). Simulating energy and carbon fluxes over winter wheat using coupled land surface and terrestrial ecosystem models. *Agricult. For. Meteorol.* 118, 21–47. doi: 10.1016/s0168-1923(03)00073-x

Atkin, O. K., Edwards, E. J., and Loveys, B. R. (2000). Response of root respiration to changes in temperature and its relevance to global warming. *New Phytol.* 147, 141–154. doi: 10.1046/j.1469-8137.2000.00683.x

Bai, J., Ouyang, H., Deng, W., Zhu, Y., Zhang, X., and Wang, Q. (2005). Spatial distribution characteristics of organic matter and total nitrogen of marsh soils in river marginal wetlands. *Geoderma* 124, 181–192. doi: 10.1016/j.geoderma.2004.04.012

Bartholomeus, R. P., Witte, J.-P. M., van Bodegom, P. M., van Dam, J. C., and Aerts, R. (2008). Critical soil conditions for oxygen stress to plant roots: substituting the feddes-function by a process-based model. *J. Hydrol.* 360, 147–165. doi: 10.1016/j.jhydrol.2008.07.029

Blom, C. (1999). Adaptations to flooding stress: from plant community to molecule. *Plant Biol.* 1, 261–273. doi: 10.1055/s-2007-978515

Blume-Werry, G., Milbau, A., Teuber, L. M., Johansson, M., and Dorrepaal, E. (2019). Dwelling in the deep–strongly increased root growth and rooting depth enhance plant interactions with thawing permafrost soil. *New Phytol.* 223, 1328–1339. doi: 10.1111/nph.15903

Booth, E. G., and Loheide, S. P. (2010). Effects of evapotranspiration partitioning, plant water stress response and topsoil removal on the soil moisture regime of a floodplain wetland: implications for restoration. *Hydrol. Process.* 24, 2934–2946. doi: 10.1002/hyp.7707

Byun, C., Nam, J. M., and Kim, J. G. (2017). Effects of flooding regime on wetland plant growth and species dominance in a mesocosm experiment. *Plant Ecol.* 218, 517–527. doi: 10.1007/s11258-017-0707-0

Caffrey, J., and Kemp, W. (1991). Seasonal and spatial patterns of oxygen production, respiration and root-rhizome release in *Potamogeton perfoliatus* l. and *Zostera marina* l. *Aquat. Bot.* 40, 109–128. doi: 10.1016/0304-3770(91)90090-R

Calleja-Cabrera, J., Boter, M., Oñate-Sánchez, L., and Pernas, M. (2020). Root growth adaptation to climate change in crops. *Front. Plant Sci.* 11:544. doi: 10.3389/fpls.2020.00544

Casanova, M. T., and Brock, M. A. (2000). How do depth, duration and frequency of flooding influence the establishment of wetland plant communities? *Plant Ecol.* 147, 237–250. doi: 10.1023/A:1009875226637

Cesarz, S., Ciobanu, M., Wright, A. J., Ebeling, A., Vogel, A., Weisser, W. W., et al. (2017). Plant species richness sustains higher trophic levels of soil nematode communities after consecutive environmental perturbations. *Oecologia* 184, 715–728. doi: 10.1007/s00442-017-3893-5

Coleman, J. M., Huh, O. K., and Braud, D. (2008). Wetland loss in world deltas. *J. Coast. Res.* 24, 1–14. doi: 10.2112/05-0607.1

Colmer, T. (2003). Long-distance transport of gases in plants: a perspective on internal aeration and radial oxygen loss from roots. *Plant Cell Environ.* 26, 17–36. doi: 10.1046/j.1365-3040.2003.00846.x

Cook, F. (1995). One-dimensional oxygen diffusion into soil with exponential respiration: analytical and numerical solutions. *Ecol. Model.* 78, 277–283. doi: 10.1016/0304-3800(94)00179-l

Dalmagro, H. J., Lathuillière, M. J., Vourlitis, G. L., Campos, R. C., Pinto, O. B. Jr., Johnson, M. S., et al. (2016). Physiological responses to extreme hydrological events in the pantanal wetland: heterogeneity of a plant community containing super-dominant species. *J. Veg. Sci.* 27, 568–577. doi: 10.1111/jvs.12379

De Willigen, P., and Van Noordwijk, M. (1984). Mathematical models on diffusion of oxygen to and within plant roots, with special emphasis on effects of soil-root contact. *Plant Soil* 77, 215–231. doi: 10.1007/bf02182925

DeLaune, R., Pezeshki, S., and Pardue, J. (1990). An oxidation-reduction buffer for evaluating the physiological response of plants to root oxygen stress. *Environ. Exp. Bot.* 30, 243–247. doi: 10.1016/0098-8472(90)90070-k

Evans, D. E. (2004). Aerenchyma formation. *New Phytol.* 161, 35–49. doi: 10.1046/j.1469-8137.2003.00907.x

Ewing, K. (1996). Tolerance of four wetland plant species to flooding and sediment deposition. *Environ. Exp. Bot.* 36, 131–146. doi: 10.1016/0098-8472(96)01000-3

Fischer, F. M., Wright, A. J., Eisenhauer, N., Ebeling, A., Roscher, C., Wagg, C., et al. (2016). Plant species richness and functional traits affect community stability after a flood event. *Philos. Transac. R. Soc. B Biol. Sci.* 371, 20150276. doi: 10.1098/rstb.2015.0276

Gardner, R. C., and Davidson, N. C. (2011). "The ramsar convention," in *Wetlands*, ed. B. LePage (Dordrecht: Springer), doi: 10.1007/978-94-007-0551-7_11.

Gattringer, J. P., Donath, T. W., Eckstein, R. L., Ludewig, K., Otte, A., and Harvolk-Schöning, S. (2017). Flooding tolerance of four floodplain meadow species depends on age. *PLoS One* 12:e0176869. doi: 10.1371/journal.pone.0176869

Gattringer, J. P., Ludewig, K., Harvolk-Schöning, S., Donath, T. W., and Otte, A. (2018). Interaction between depth and duration matters: flooding tolerance of 12 floodplain meadow species. *Plant Ecol.* 219, 973–984. doi: 10.1007/s11258-018-0850-2

Glenz, C., Schlaepfer, R., Iorgulescu, I., and Kienast, F. (2006). Flooding tolerance of central european tree and shrub species. *For. Ecol. Manag.* 235, 1–13. doi: 10.1016/j.foreco.2006.05.065

Haak, D. C., Fukao, T., Grene, R., Hua, Z., Ivanov, R., Perrella, G., et al. (2017). Multilevel regulation of abiotic stress responses in plants. *Front. Plant Sci.* 8:1564. doi: 10.3389/fpls.2017.01564

Hammersley, J. (2013). *Monte Carlo Methods*. Berlin: Springer Science & Business Media. doi: 10.1007/978-94-009-5819-7.

Hough-Snee, N., Nackley, L. L., Kim, S.-H., and Ewing, K. (2015). Does plant performance under stress explain divergent life history strategies? The effects of flooding and nutrient stress on two wetland sedges. *Aquat. Bot.* 120, 151–159. doi: 10.1016/j.aquabot.2014.03.001

Isbell, F., Craven, D., Connolly, J., Loreau, M., Schmid, B., Beierkuhnlein, C., et al. (2015). Biodiversity increases the resistance of ecosystem productivity to climate extremes. *Nature* 526:574. doi: 10.1038/nature15374

Jackson, M., and Armstrong, W. (1999). Formation of aerenchyma and the processes of plant ventilation in relation to soil flooding and submergence. *Plant Biol.* 1, 274–287. doi: 10.1111/j.1438-8677.1999.tb00253.x

Jones, C. G., Lawton, J. H., and Shachak, M. (1994). "Organisms as ecosystem engineers," in *Ecosystem Management*, eds F.B. Samson and F. L. Knopf (New York, NY: Springer), doi: 10.1007/978-1-4612-4018-1_14.

Jung, V., Hoffmann, L., and Muller, S. (2008). "Ecophysiological responses of nine floodplain meadow species to changing hydrological conditions," in *Herbaceous Plant Ecology*, ed. A. G. Van der Valk (Dordrecht: Springer). doi: 10.1007/978-90-481-2798-6_18

Kirwan, M. L., and Guntenspergen, G. R. (2015). Response of plant productivity to experimental flooding in a stable and a submerging marsh. *Ecosystems* 18, 903–913. doi: 10.1007/s10021-015-9870-0

Kozlowski, T. T. (2002). Physiological-ecological impacts of flooding on riparian forest ecosystems. *Wetlands* 22, 550–561. doi: 10.1672/0277-5212(2002)022[0550:PEIOFO]2.0.CO;2

Kumari, A., and Gupta, K. J. (2017). "Visisens technique to measure internal oxygen and respiration in barley roots," in *Plant Respiration and Internal Oxygen*, ed. J. G. Kapuganti (New York, NY: Springer), doi: 10.1007/978-1-4939-7292-0_4.

Laan, P., Berrevoets, M., Lythe, S., Armstrong, W., and Blom, C. (1989). Root morphology and aerenchyma formation as indicators of the flood-tolerance of rumex species. *J. Ecol.* 77, 693–703. doi: 10.2307/2260979

Lai, W.-L., Zhang, Y., and Chen, Z.-H. (2012). Radial oxygen loss, photosynthesis, and nutrient removal of 35 wetland plants. *Ecol. Eng.* 39, 24–30. doi: 10.1016/j.ecoleng.2011.11.010

Lai, Z., Lu, S., Zhang, Y., Wu, B., Qin, S., Feng, W., et al. (2016). Diel patterns of fine root respiration in a dryland shrub, measured in situ over different phenological stages. *J. For. Res.* 21, 31–42. doi: 10.1007/s10310-015-0511-4

Lemon, E., and Wiegand, C. (1962). Soil aeration and plant root relations ii. Root respiration 1. *Agron. J.* 54, 171–175. doi: 10.2134/agronj1962.00021962005400020024x

Li, S., Zhou, D., Luan, Z., Pan, Y., and Jiao, C. (2011). Quantitative simulation on soil moisture contents of two typical vegetation communities in Sanjiang Plain, China. *Chinese Geogr. Sci.* 21, 723–733. doi: 10.1007/s11769-011-0507-8

Maricle, B. R., and Lee, R. W. (2002). Aerenchyma development and oxygen transport in the estuarine cordgrasses *Spartina alterniflora* and *S. Anglica*. *Aquat. Bot.* 74, 109–120. doi: 10.1016/S0304-3770(02)00051-7

Montagnoli, A., Terzaghi, M., Chiatante, D., Scippa, G. S., Lasserre, B., and Dumroese, R. K. (2019). Ongoing modifications to root system architecture of pinus ponderosa growing on a sloped site revealed by tree-ring analysis. *Dendrochronologia* 58:125650. doi: 10.1016/j.dendro.2019.125650

Myers-Smith, I. H., Elmendorf, S. C., Beck, P. S., Wilmking, M., Hallinger, M., Blok, D., et al. (2015). Climate sensitivity of shrub growth across the tundra biome. *Nat. Clim. Change* 5, 887–891. doi: 10.1038/nclimate2697

Niu, Z., Zhang, H., Wang, X., Yao, W., Zhou, D., Zhao, K., et al. (2012). Mapping wetland changes in China between 1978 and 2008. *Chinese Sci. Bull.* 57, 2813–2823. doi: 10.1007/s11434-012-5093-3

Pedersen, O., Perata, P., and Voesenek, L. A. (2017). Flooding and low oxygen responses in plants. *Funct. Plant Biol.* 44, iii–vi. doi: 10.1071/fpv44n9_fo

Pedersen, O., Sand-Jensen , K., and Revsbech, N. P. (1995). Diel pulses of o_2 and co_2 in sandy lake sediments inhabited by lobelia dortmanna. *Ecology* 76, 1536–1545. doi: 10.2307/1938155

Pezeshki, S. (1998). Photosynthesis and root growth in spartina alterniflora in relation to root zone aeration. *Photosynthetica* 34, 107–114. doi: 10.1023/a:1006820019220

Pezeshki, S. (2001). Wetland plant responses to soil flooding. *Environ. Exp. Bot.* 46, 299–312. doi: 10.1016/s0098-8472(01)00107-1

Pezeshki, S. R., Finlayson, C. M., Everard, M., Irvine, K., Mcinnes, R. J., Middleton, B. A., et al. (eds) (2018). "Photosynthesis in wetlands," in *The Wetland Book: I: Structure and Function, Management, and Methods*, (Dordrecht: Springer Netherlands). doi: 10.1007/978-90-481-9659-3_64.

Pezeshki, S., DeLaune, R., and Patrick, W. Jr. (1987). Effects of flooding and salinity on photosynthesis of *Sagittaria lancifolia*. *Mar. Ecol. Progr. Ser.* 41, 87–91. doi: 10.3354/meps041087

Pregitzer, K. S., King, J. S., Burton, A. J., and Brown, S. E. (2000). Responses of tree fine roots to temperature. *New Phytol.* 147, 105–115. doi: 10.1046/j.1469-8137.2000.00689.x

Probert, M., Dimes, J., Keating, B., Dalal, R., and Strong, W. (1998). Apsim's water and nitrogen modules and simulation of the dynamics of water and nitrogen in fallow systems. *Agricult. Syst.* 56, 1–28. doi: 10.1016/s0308-521x(97)00028-0

Purcell, A. S., Lee, W. G., Tanentzap, A. J., and Laughlin, D. C. (2019). Fine root traits are correlated with flooding duration while aboveground traits are related to grazing in an ephemeral wetland. *Wetlands* 39, 291–302. doi: 10.1007/s13157-018-1084-8

Reddy, K. R., and DeLaune, R. D. (2008). *Biogeochemistry of Wetlands: Science and Applications*. Boca Raton, FL: CRC press. doi: 10.1201/9780203491454.

Reich, P. B., Knops, J., Tilman, D., Craine, J., Ellsworth, D., Tjoelker, M., et al. (2001). Plant diversity enhances ecosystem responses to elevated CO_2 and nitrogen deposition. *Nature* 410:809. doi: 10.1038/35081122

Rubol, S., Silver, W. L., and Bellin, A. (2012). Hydrologic control on redox and nitrogen dynamics in a peatland soil. *Sci. Total Environ.* 432, 37–46. doi: 10.1016/j.scitotenv.2012.05.073

Simunek, J., Van Genuchten, M. T., and Sejna, M. (2005). *The HYDRUS-1D Software Package for Simulating the One-Dimensional Movement of Water, Heat, and Multiple Solutes in Variably-Saturated Media. Version 3.0. HYDRUS Software Series 1*. Riverside*:* University of California Riverside, 1-240.

Striker, G., Insausti, P., Grimoldi, A., and Vega, A. (2007). Trade-off between root porosity and mechanical strength in species with different types of aerenchyma. *Plant Cell Environ.* 30, 580–589. doi: 10.1111/j.1365-3040.2007.01639.x

Van Genuchten, M. T. (1980). A closed-form equation for predicting the hydraulic conductivity of unsaturated soils 1. *Soil Sci. Soc. Am. J.* 44, 892–898. doi: 10.2136/sssaj1980.03615995004400050002x

Watanabe, K., Takahashi, H., Sato, S., Nishiuchi, S., Omori, F., Malik, A. I., et al. (2017). A major locus involved in the formation of the radial oxygen loss barrier in adventitious roots of teosinte zea nicaraguensis is located on the short-arm of chromosome 3. *Plant Cell Environ.* 40, 304–316. doi: 10.1111/pce.12849

Waters, I., Armstrong, W., Thompson, C., Setter, T., Adkins, S., Gibbs, J., et al. (1989). Diurnal changes in radial oxygen loss and ethanol metabolism in roots of submerged and non-submerged rice seedlings. *New Phytol.* 113, 439–451. doi: 10.1111/j.1469-8137.1989.tb00355.x

Watson, E. B., Andrews, H. M., Fischer, A., Cencer, M., Coiro, L., Kelley, S., et al. (2015). Growth and photosynthesis responses of two co-occurring marsh grasses to inundation and varied nutrients. *Botany* 93, 671–683. doi: 10.1139/cjb-2015-0055

Weiss, R. F. (1970). The solubility of nitrogen, oxygen and argon in water and seawater. *Deep Sea Res. Oceanogr. Abstracts.* 17, 721–735. doi: 10.1016/0011-7471(70)90037-9

Wright, A. J., de Kroon, H., Visser, E. J. W., Buchmann, T., Ebeling, A., Eisenhauer, N., et al. (2017). Plants are less negatively affected by flooding when growing in species-rich plant communities. *New Phytol.* 213, 645–656. doi: 10.1111/nph.14185

Wright, A. J., Ebeling, A., De Kroon, H., Roscher, C., Weigelt, A., Buchmann, N., et al. (2015). Flooding disturbances increase resource availability and productivity but reduce stability in diverse plant communities. *Nat. Commun.* 6:6092. doi: 10.1038/ncomms7092

Yamauchi, T., Colmer, T. D., Pedersen, O., and Nakazono, M. (2018). Regulation of root traits for internal aeration and tolerance to soil waterlogging-flooding stress. *Plant Physiol.* 176, 1118–1130. doi: 10.1104/pp.17.01157

Yan, K., Zhao, S., Cui, M., Han, G., and Wen, P. (2018). Vulnerability of photosynthesis and photosystem i in Jerusalem artichoke (*Helianthus tuberosus* l.) exposed to waterlogging. *Plant Physiol. Biochem.* 125, 239–246. doi: 10.1016/j.plaphy.2018.02.017

Zeng, Y. (eds) (2013). "Diurnal pattern of coupled moisture and heat transport process," in *Coupled Dynamics in Soil*, (New York, NY: Springer), doi: 10.1007/978-3-642-34073-4_2.

Zeng, Y., Su, Z., Wan, L., and Wen, J. (2011). A simulation analysis of the advective effect on evaporation using a two-phase heat and mass flow model. *Water Resourc. Res.* 47:W10529. doi: 10.1029/2011WR010701

Zhang, D., Qi, Q., Wang, X., Tong, S., Lv, X., An, Y., et al. (2019). Physiological responses of *Carex schmidtii* meinsh to alternating flooding-drought conditions in the Momoge wetland, Northeast China. *Aquat. Bot.* 153, 33–39. doi: 10.1016/j.aquabot.2018.11.010

Zhang, Y., Niu, J., Yu, X., Zhu, W., and Du, X. (2015). Effects of fine root length density and root biomass on soil preferential flow in forest ecosystems. *For. Syst.* 24:12. doi: 10.5424/fs/2015241-06048

Zhou, D., Gong, H., Wang, Y., Khan, S., and Zhao, K. (2009). Driving forces for the marsh wetland degradation in the honghe national nature reserve in Sanjiang Plain, Northeast China. *Environ. Model. Assess.* 14, 101–111. doi: 10.1007/s10666-007-9135-1

Zhou, D., Wang, Z., Tang, T., Li, S., and Liu, C. (2013). Prediction of the changes in ecological pattern of wetlands due to a new dam establishment in China. *Ecohydrol. Hydrobiol.* 13, 52–61. doi: 10.1016/j.ecohyd.2013.03.002

Zhou, D., Zhang, H., and Liu, C. (2016). Wetland ecohydrology and its challenges. *Ecohydrol. Hydrobiol.* 16, 26–32. doi: 10.1016/j.ecohyd.2015.08.004

Conflict of Interest: The authors declare that the research was conducted in the absence of any commercial or financial relationships that could be construed as a potential conflict of interest.

Publisher's Note: All claims expressed in this article are solely those of the authors and do not necessarily represent those of their affiliated organizations, or those of the publisher, the editors and the reviewers. Any product that may be evaluated in this article, or claim that may be made by its manufacturer, is not guaranteed or endorsed by the publisher.